京都大学防災研究所年報 第 62 号 B
DPRI Annuals, No. 62 B, 2019

Numerical Study on the Hydro-Morphological and Bank Erosion Characteristics of Uji River, Japan

Saroj KARKI [(1)], Hajime NAKAGAWA[(2)], Kenji KAWAIKE[(2)] and Masakazu HASHIMOTO[(3)]

(1) Department of Civil and Earth Resources Engineering, Kyoto University
(2) Disaster Prevention Research Institute (DPRI), Kyoto University
(3) International Research Institute of Disaster Science (IRIDeS), Tohoku University

Synopsis

We performed numerical study on Uji River with an objective to analyze the channel hydro-morphological characteristics including bank erosion process. Simulation results suggested that the overall channel evolution is insignificant but the bank erosion is dominant at several locations. It was also concluded that the bank erosion is mainly caused by the undercutting of the bank toe due to the low flow condition which induce high bed shear stress and high near bank velocity. With higher flow discharge, the zone of maximum velocity tend to shift more towards the channel center. Results of the prediction of bank erosion indicated that fluvial erosion due to the scour near the bank toe is dominant at most of the locations in Uji River.

Keywords: alluvial meanders, Uji River, bank erosion, numerical simulation, telemac-2d

1. INTRODUCTION

Evolution of Rivers through erosion-deposition processes is a continuous phenomenon especially in alluvial meandering channels. While rivers have been utilized to serve various human-related purposes but lack of their proper management, have resulted in adverse impact such as flooding, bank erosion and channel migration. Therefore studies on the river hydro-morphology have been a subject of great interest for river morphologists, scientists, engineers and a challenge at the same. They recognize that any engineering effort in rivers must be based on a proper understanding of the morphological characteristics (Chang, 2008). Understanding the hydro-morphological behavior of a river channel is vital in the design and implementation of appropriate countermeasures against riverbank erosion. River bank erosion can eventually lead to channel migration, which can be difficult to predict accurately. For this reason, river erosion and migration can pose substantial risks to existing infrastructures such as houses, agricultural land, roads and bridges years after their construction (Lagasse et al., 2004)

In this regard, the current study aims to investigate the hydro-morphological characteristics of Uji River in Kyoto, Japan with an objective to identify the potential locations vulnerable to bank erosion through numerical simulation. A 2D hydro-morphological model is applied to the study reach for characterizing the channel hydro-morphology and hence identify susceptible locations of bank erosion. River morphology is influenced by several factors: change in flow discharge, flood events, alteration in sediment supply and human interventions to name a few. Changes in river morphology directly impact the

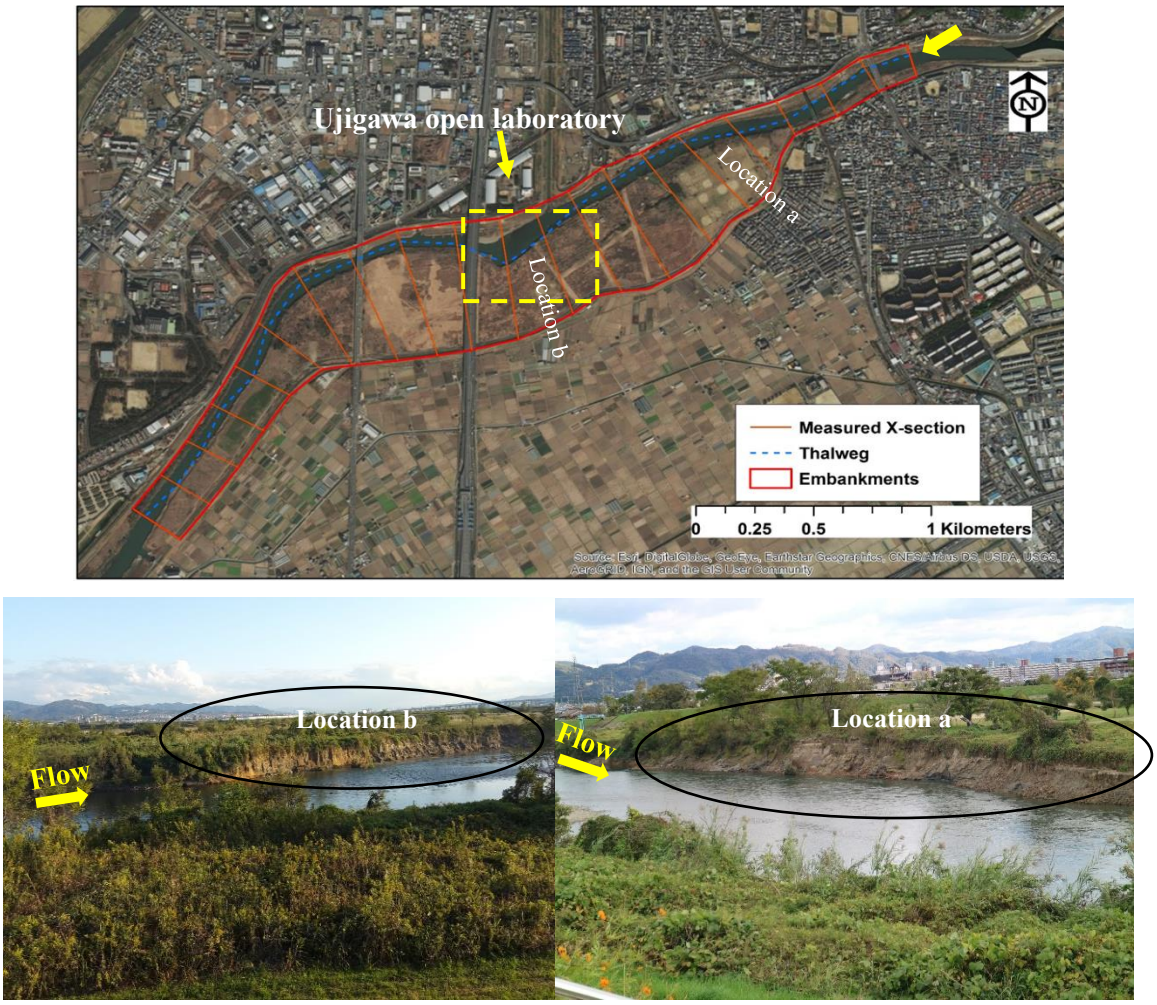

Photo 1: Location of the study domain including bank erosion

channel width adjustment process through riverbank erosion. Therefore, understanding the changes in river channel hydro-morphology is vital for maintaining stable channel sections and hence the long-term river management. In this context, this study intends to study the hydro-morphological and bank erosion characteristics of Uji River using depth averaged 2D coupled model of flow and bed morphology. Additionally river bank erosion of selected locations are also analyzed through bank erosion model.

2. STUDY AREA

The river reaches selected for the current study as shown in Photo 1 is the Uji River beginning from the confluence with Yamashina River near Mukaijima to about 4km downstream. The curved portion near the Ujigawa Open laboratory is analyzed in detail because of the severity of bank erosion along that bend.

3. MODEL DESCRIPTION

An open source depth-averaged hydrodynamic model Telemac-2D coupled internally with the sediment transport model Sisyphe from the TELEMAC-MASCARET suite of solvers (www.opentelemac.org) was applied to study the channel hydrodynamics and morphological changes. Telemac-2D solves the shallow water equations (momentum and continuity) using the finite-element in an unstructured (triangular elements) computational mesh. The sediment transport model Sisyphe and the hydrodynamic model Telemac-2D are internally coupled where at each time step, Sisyphe receives the spatial distribution of the main hydrodynamic variables: water depth h, horizontal depth-averaged flow velocity components V_x and V_y, and bed shear stress τ calculated by the hydrodynamic model. Telemac-2D has been validated for various analytical,

experimental and real-field cases (Hervouet & Bates, 2000).

3.1 Hydrodynamic model

Telemac-2D solves the depth-averaged RANS equations as shown in Eq. [1-3]. In this study, the k-ϵ turbulence model was used.

$$\frac{\partial h}{\partial t} + \frac{\partial (hV_x)}{\partial x} + \frac{\partial (hV_y)}{\partial y} = 0 \qquad [1]$$

$$\frac{\partial V_x}{\partial t} + V_x \frac{\partial (V_x)}{\partial x} + V_y \frac{\partial (V_x)}{\partial y} = -g \frac{\partial Z_s}{\partial x} + F_x + \frac{1}{h} \nabla [h v_T \vec{\nabla}(V_x)] \quad [2]$$

$$\frac{\partial V_y}{\partial t} + V_x \frac{\partial (V_y)}{\partial x} + V_y \frac{\partial (V_y)}{\partial y} = -g \frac{\partial Z_s}{\partial x} + F_x + \frac{1}{h} \nabla [h v_T \vec{\nabla}(V_y)] \quad [3]$$

where,

t = time

x, y = horizontal Cartesian coordinates

Z_s = water surface

v_T= turbulent viscosity

F_x, F_y = source terms which includes friction forces

3.2 Sediment transport and bed evolution model

In the current study, we considered a non-uniform sediment transport using the active layer concept (Hirano, 1971). The uppermost bed layer is subdivided into two layers: an active layer which is in contact with the flow, and a substrate layer directly below. The active layer supplies sediment to be transported as bed load as well as receives the sediment for deposition. The role of the lower substratum layer is to exchange sediment with the active layer so as to maintain its thickness. The sediment material is divided into N size-fractions (five size-class in this study), each characterized by a diameter, d_k, and a volume percentage of occurrence, p_k. The sediment transport is assumed to adapt instantaneously to the driving hydrodynamics and is computed according to the availability of each grain size fraction (El Kadi Abderrezzak et al. 2016). The bed load rate per unit width for the kth fraction size, q_{bk}, was calculated using the Meyer-Peter and Müller (1948) empirical formula and weighted depending on the proportion of the k_{th} fraction in the sediment mix. Modifications of the critical shield's parameter due to hiding/exposure effect was calculated using Ashida-Michiue's (1973) formula. The magnitude and direction of the bed load are influenced by the transverse bed slope. We used Koch & Flokstra (1980) formulation to account for this effect. The bed evolution was calculated using Exner formula.

$$(1-p)\left(\frac{\partial z_b}{\partial t}\right)_k + \frac{\partial (q_{bk} \cos \alpha_k)}{\partial x} + \frac{\partial (q_{bk} \sin \alpha_k)}{\partial y} = 0 \quad [4]$$

Where,

p = porosity of bed material

α_k = angle between the bedload direction and the x-axis

$\left(\frac{\partial z_b}{\partial t}\right)_k$= rate of change in bed elevation corresponding to the kth fraction size.

To account for the effect of secondary currents in curved channels, Engelund's (1974) formulation has been incorporated. The transverse bed evolution in curved channels can be well reproduced in 2D models using this formulation. The direction of bed shear stress relative to the flow direction is modified depending on the water-depth h, and the local radius of curvature, R_c. The radius, unknown in the model, can be substituted using the formulation for the slope of the free surface, $\partial Z_s/\partial y$ such that $g\,(\partial Z_s/\partial y) = \alpha' U^2/R_c$ in bends. The correction factor α' is the only calibration parameter and should be chosen between 0.75, in the presence of bedforms, and 1, for flat-bed conditions which was considered in this study (Villaret et al., 2013)

4. INPUT DATA

In order to set-up the model for simulation, we needed to carefully prepare different types of input data. Different data used for the simulation are discussed in brief in the next sections.

4.1 River Bathymetry

River bathymetry was generated by the spatial interpolation of the cross-sections data obtained from the Ministry of Land Infrastructure and Transport, Japan. The cross-sections data were recorded at the end of the year 2015. Fig.1 shows the channel bathymetry data within the study domain. River profile and typical cross-section are shown in inside the rectangle in Fig.1. For the spatial interpolation, we used HEC-GeoRAS application in ArcGIS interface.

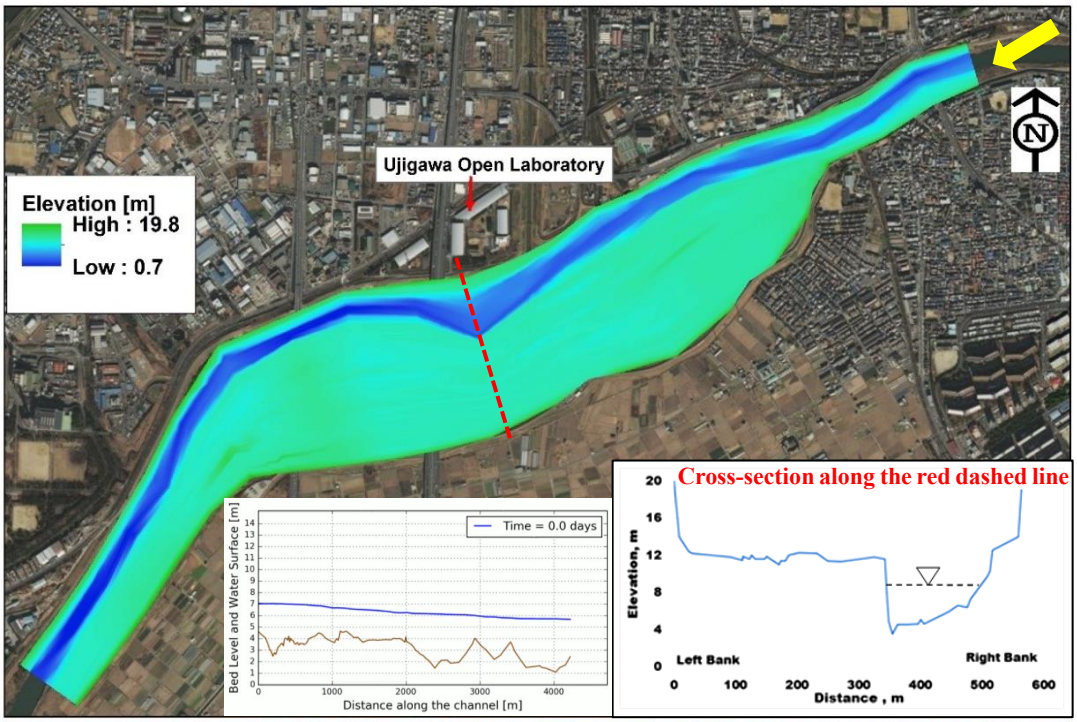

Fig.1: Channel bathymetry, longitudinal profile and typical cross-section

4.2 Inflow Discharge and Water Level and Sediment

The inflow and outflow boundary for the model was given as the observed discharge and the observed water-level respectively. Since the river bathymetry was taken at the end of 2015, measured flow and water-level data of the year 2016 at Kumiyama-cho, Ohashiberi, Kyoto observing station were used for the simulation. The graph in Fig. 2 shows the observed discharge and water level for one year period of 2016. These data show highly regulated flows due to the operation of Amagashe dam in the upstream of Uji River.

Sediment samples of the river-bed were collected from the top of the point bar at two different locations and sieve analysis was performed on the collected sediment samples. Fig.3 (a & b) shows the particle size distribution curve of the two samples.

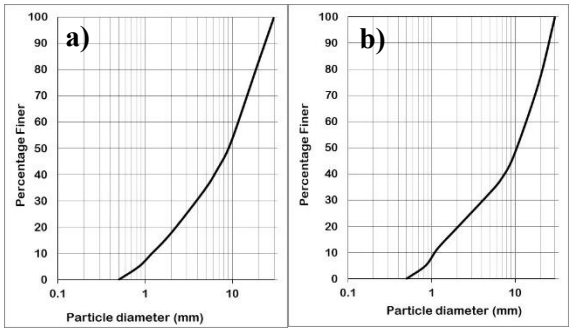

Fig.3: Particle size distribution curve

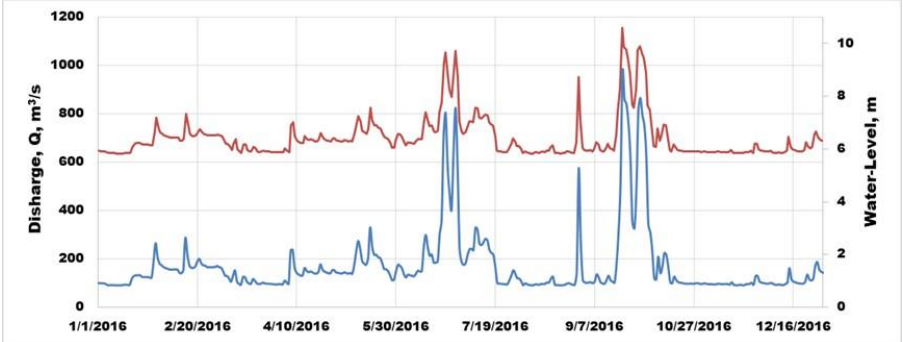

Fig.2: Observed water-level and inflow discharge used in the simulation

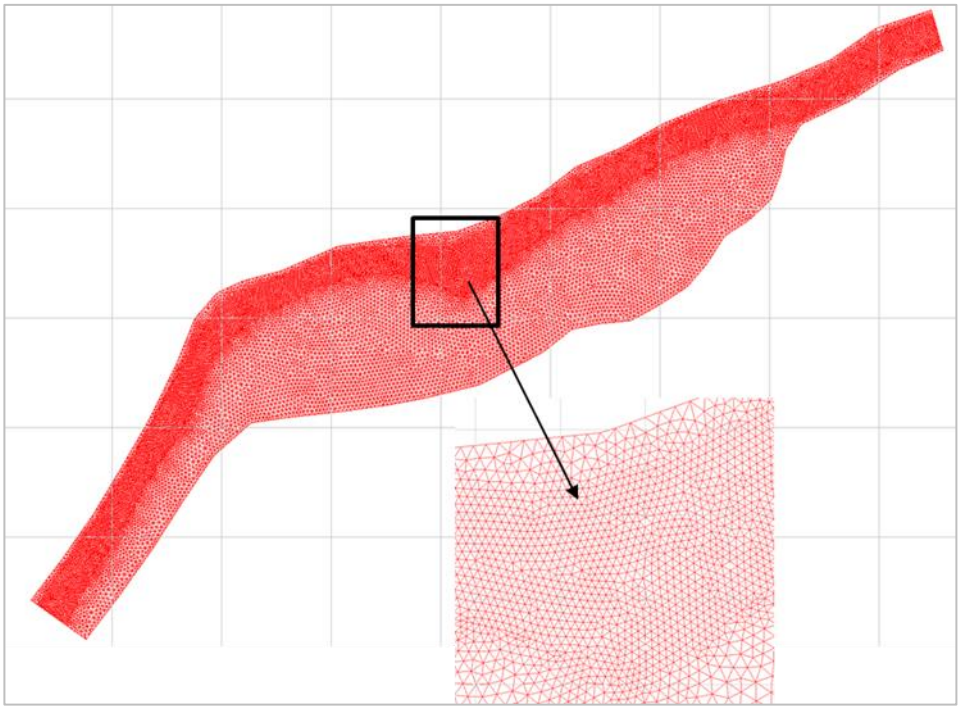

Fig.4: Unstructured mesh generated for the study domain

4.3 Model Calibration

After preparing the required input data, the model was set-up. Fig. 4 illustrates the mesh generated for the study reach. The simulation was first run under fixed-bed case for the calibration of the model. And in the next case, with a movable bed and finally the bank erosion case was performed.

The purpose of the fixed-bed simulation was to calibrate the model. The results of the simulation showed good agreement with the observed data as shown in Fig.5. The R^2 values for both the discharge and the water level are greater than 0.99. This simulation of fixed bed case shows the model capability to compute the hydrodynamic variables under a range of inflow discharges. A typical water-surface profile is shown in Fig.6 for the *50*th day of simulation with an inflow discharge of about 200m^3/s. The difference in the water level between the upstream and the downstream boundary is about 1m.

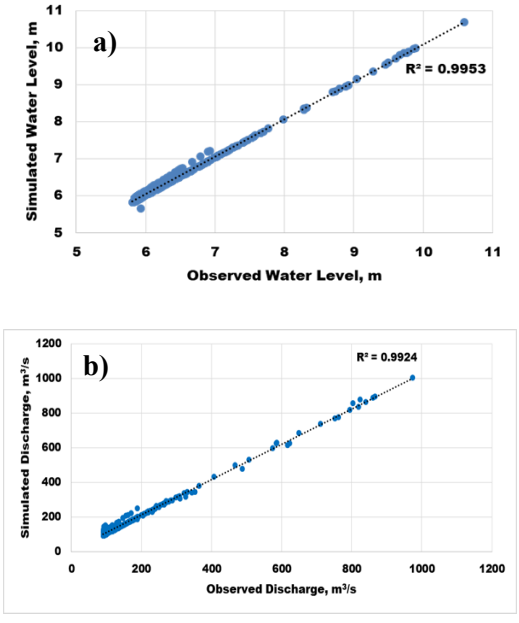

Fig.5: Calibration of a) water-level and b) discharge

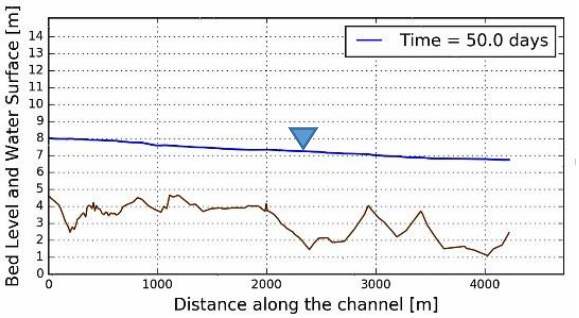

Fig.6: Water surface profile at 50th day of simulation [Q=200m^3/s]

5. SIMULATION RESULTS

In the next step, we considered sediment transport with an objective to identify the channel morphological changes. However, the bed evolution

was almost negligible. This might be due to the effect of coarser bed materials used in the simulation. Since the sediment sample was collected from the point bar instead of the actual river-bed. The other reason might be due to the bed armouring process caused by the reduction of sediment supply by Amagashe dam.

Fig.7 depicts the depth-averaged velocity distribution corresponding to two different flow conditions a)low flow (Q=97m^3/s) and b) high flow (Q=584m^3/s). It can be seen that the streamlines are more oriented towards the bank during the low flow while during the high flow, higher velocity flow is

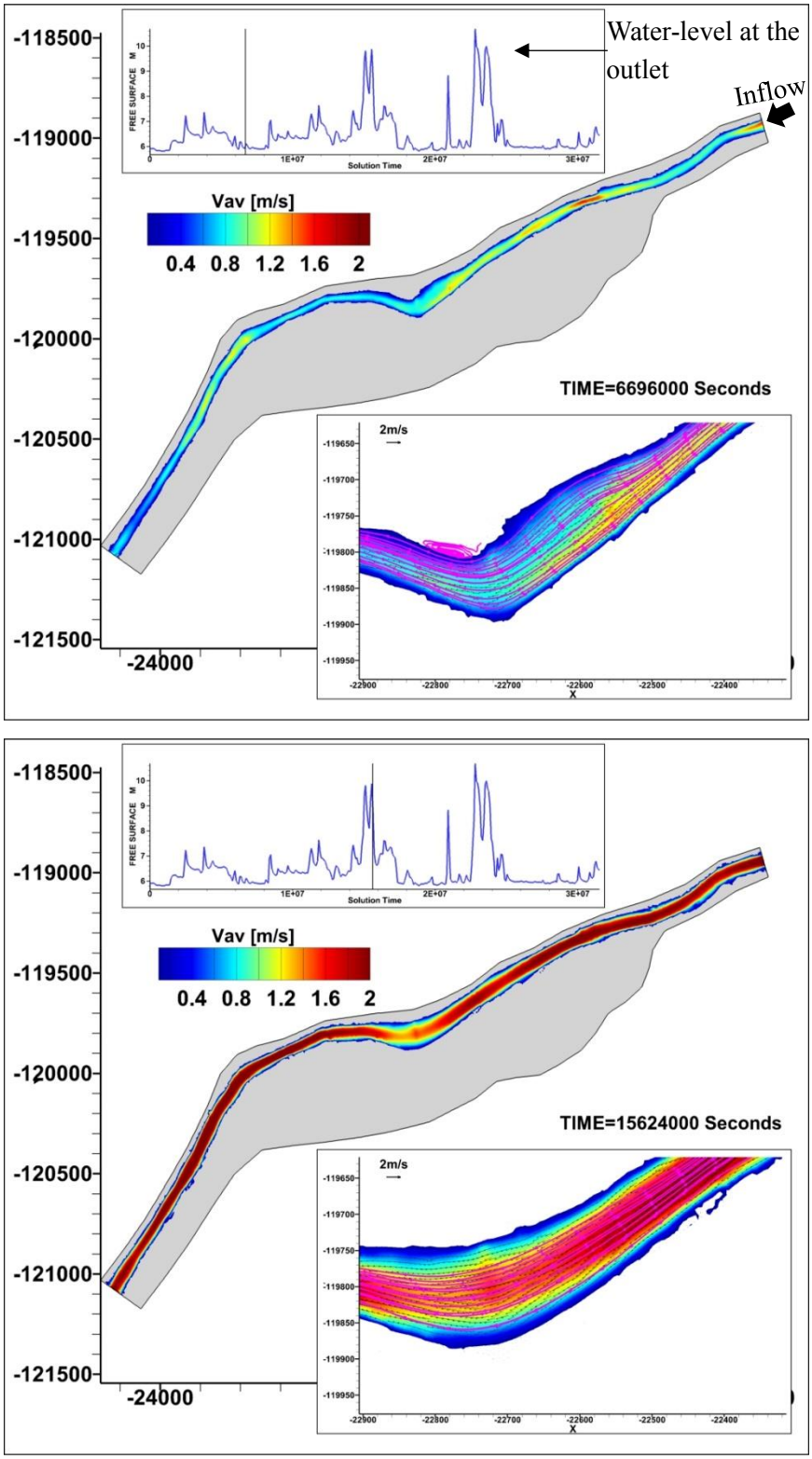

Fig.7: Depth-averaged velocity distribution for a) low-flow and b)high flow condition

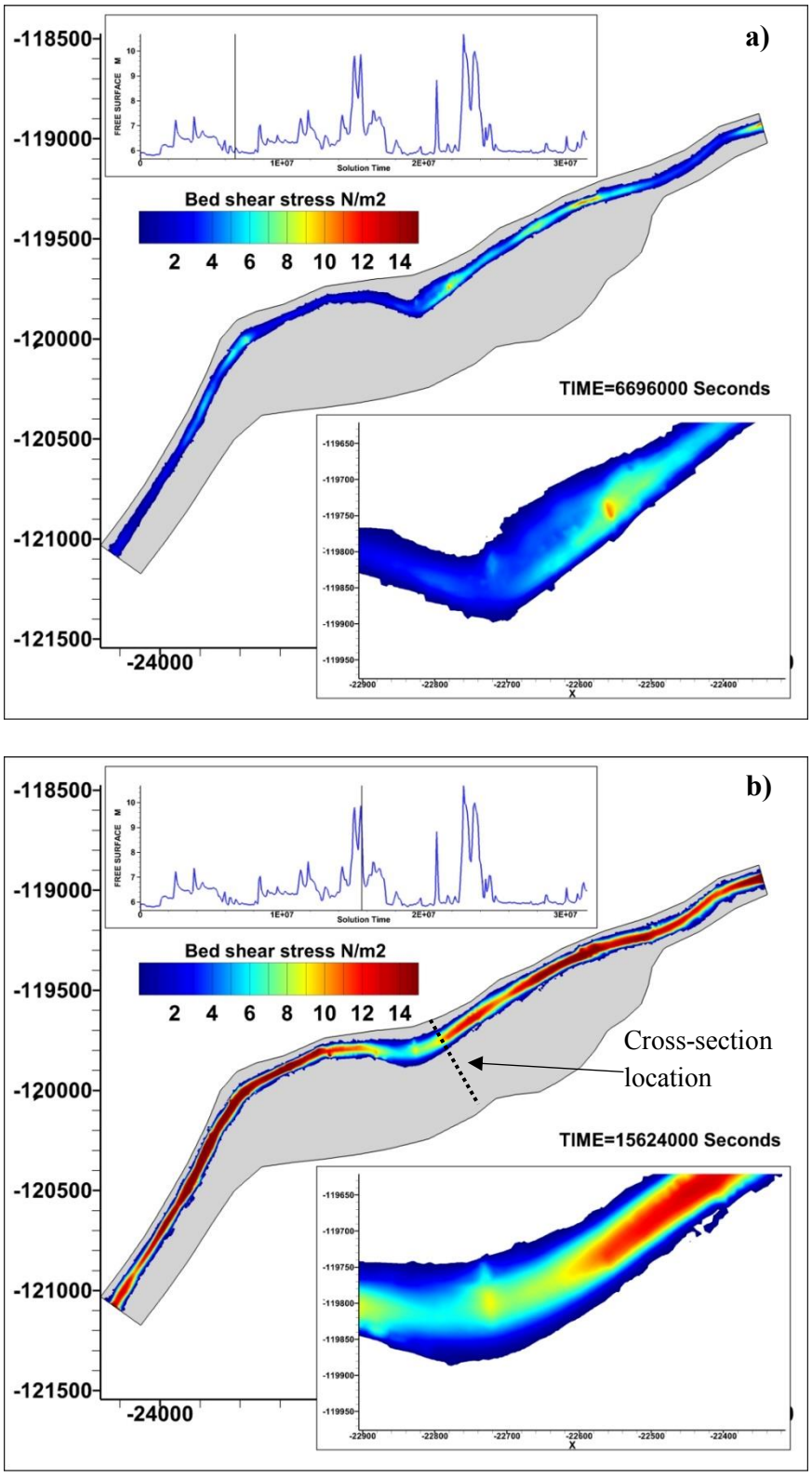

Fig. 8: Bed shear stress (τ) distribution for a) low flow b) high-flow condition

concentrated towards the channel center. The graph inside the rectangular box in Fig. 7 and 8 represent the water-level at the outlet i.e. downstream boundary. Similarly, Fig. 8 illustrates the distribution of bed shear stress (τ) for the low flow (Q=97m^3/s) and high-flow (Q=584m^3/s) condition. It can be observed during the low flow condition, higher bed shear stress zones are located closer to the banks.

This is due to the fact that the flow alignment is close to the banks where the channel bed elevation is lower. On the other hand, during the high flow, the higher bed shear stress zones are uniformly distributed across the channel or more along the channel center. The implication of this result is that the erosion of banks are most likely to be caused by the low flow condition rather than the high flow. Also during the receding period from high to low flow, there can be sudden change in the bed shear stress which might result in the bank failure. Therefore while implementing the bank protection works, both high & low flow phenomena should be considered.

In order to more clearly understand this phenomena, we plotted the cross-sectional distribution of depth-averaged velocity and bed shear stress as represented by Fig. 9a and 9b respectively. The location of the cross-section is shown by dashed line in Fig. 8. As mentioned above, it can be clearly seen that for the low flow condition, both near-bank bed shear stress and the velocity are greater than that for the high flow condition. The higher bed shear-stress and velocity shifts towards the channel center with increasing inflow discharge.

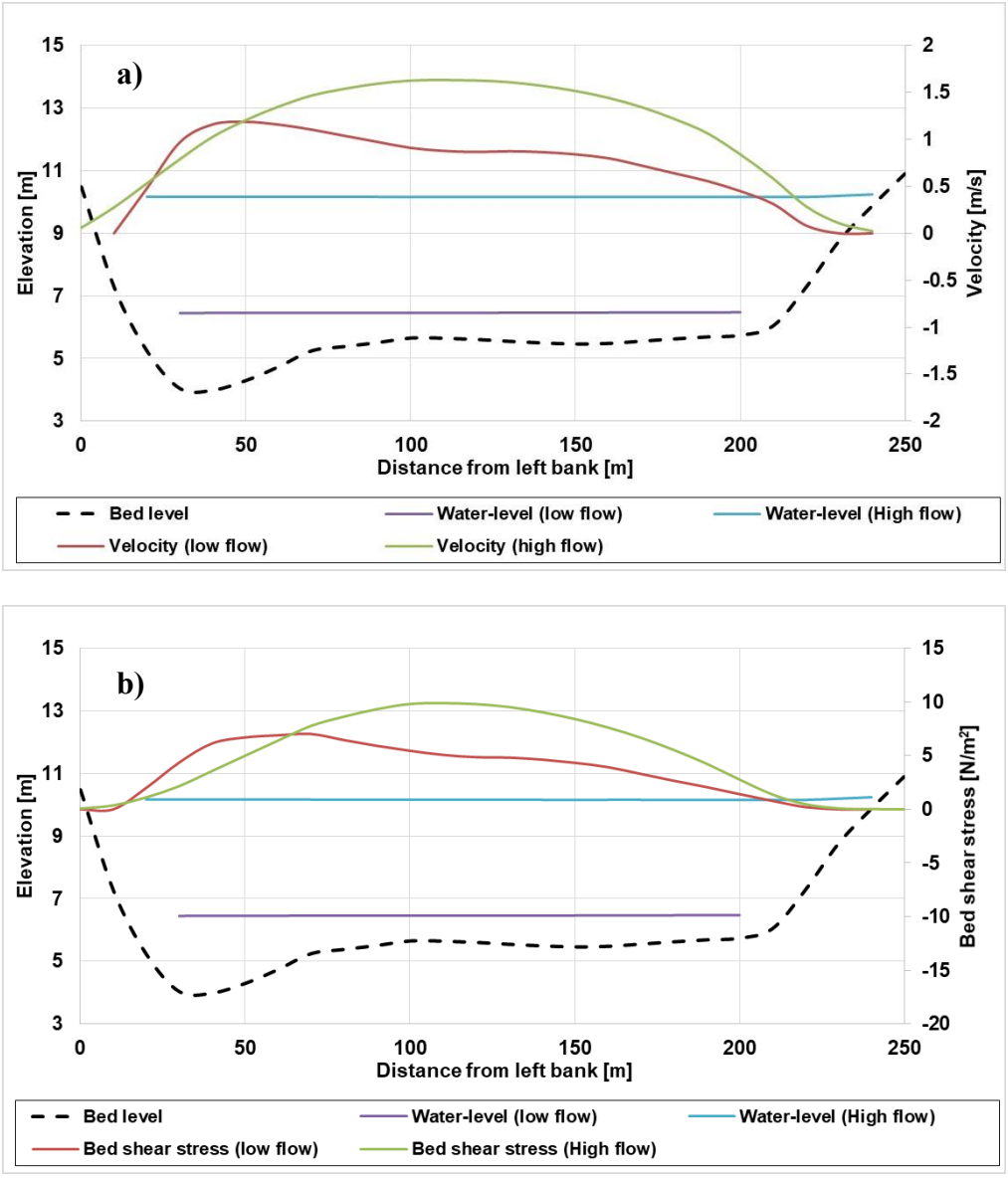

Fig. 9: Cross-sectional variation of a) depth-averaged velocity b) bed shear stress

However, results showed that the overall channel evolution is insignificant in the Uji River. The reason behind this is the channel degradation that has been caused due to the construction of Amagashe dam in the

upstream. The Amagashe dam cut the sediment supply to the river downstream. Consequently, the river degraded to such an extent that further river bed change became insignificant. This can be more clearly seen from the river profile data of the Uji River in Fig. 6. The other reason might be the sediment size that we prescribed to the model which were relatively coarser. The shear stress necessary for the transport of such coarser materials could not be exceeded.

6. Bank erosion prediction in Uji River

6.1 Satellite Imagery Analysis of Channel changes

Analysis of the river bank line changes and the corresponding areas eroded for this particular location are presented in Fig.10 and Fig.11. It can be that continuous erosion has occurred along the outer bank while the point bar has formed along the inner bank.

Fig.10 (a-e): Bankline change due to erosion of banks

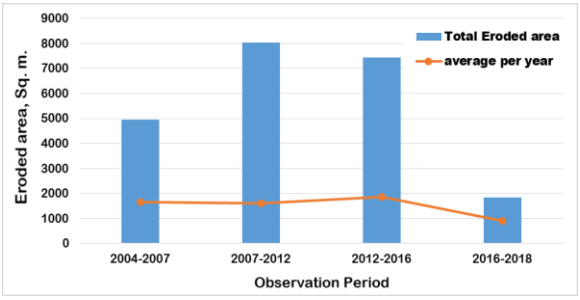

Fig.11: Rate of Bank erosion at the channel bend

In the 2D simulation of bed evolution, we identified that the overall channel evolution was insignificant along the study reach. However, it was observed from satellite imagery analysis that bank erosion at several locations is severe along the study reach. Therefore predicting the bank failure would be vital in the appropriate planning and implementation of bank erosion control measures. In this context, we made an effort to apply a bank erosion model to the study reach with an objective to check the dominant mode of bank erosion as well as evaluate model capability in predicting the bank erosion processes. In this regard, several bank failure algorithms have been formulated ranging from the simplified angle of repose approach to the more complex physically based models (El Kadi Abderrezzak et al., 2016;). Among various bank erosion models, Bank Stability and Toe Erosion Model (BSTEM) is a widely used model developed by the National Sedimentation Laboratory in Oxford, Mississippi, USA (Langendoen and Simon, 2008; Simon et al., 2010, 2000). A brief introduction on the science behind the BSTEM model and its application to the Uji River is presented in this section.

6.2 Bank erosion model

BSTEM couples iterative planar bank failure analysis based on a fundamental force balance with a toe scour model that considers the interaction between the hydrodynamics and the toe scour/deposition. The two major modes of bank failure algorithms embedded into BSTEM are:

a) Bank Failure

Bank failure mode accounts for the geotechnical failure which computes a number of failure planes as required through the bank to determine if the gravitational forces exceed the resisting frictional forces. The bank stability model performs a series of iteration to select probable failure planes, calculate the factor of safety and converge on the most likely failure plane using the following steps (CEIWR-HEC, 2015):

i) Determine the factor of safety (FS) for nodes at several vertical points on the channel bank.

ii) Compute critical factor of safety, FS_{cr}) for each vertical location after selecting the bounding failure planes (minimum and maximum angle)

iii) Select the most probable critical failure planes (FS_i~FS_{cr})

iv) Use the above information to update the critical failure plane ($FS_{i+1} \rightarrow FS_{cr}$)

v) Decide when the FS is close to FS_{cr} to stop

vi) If FS_{cr} is less than 1, fail the bank, update the cross-section, and supply the sediments to the channel for transport.

We used Layer method to compute the FS of a failure plane through the bank. In this method a non-iterative equation [**Eq. 4**] is solved to determine the FS which compares the disturbing or driving force to the balancing or resisting force.

$$FS = \frac{\sum_{i=1}^{I} c_i' L_i + S_i tan\emptyset_i^b + [W_i cos\beta - U_i + P_i \cos(\alpha - \beta)] tan\emptyset_i'}{\sum_{i=1}^{I} (W_i sin\beta - P_i \sin[\alpha - \beta])} \quad [5]$$

i=layer

L=length of failure plane

S=matrix suction force

U=hydrostatic lift

P=hydrostatic confining force of the water in the channel

$\emptyset'$= friction angle

$\emptyset^b$= relationship between matrix suction and apparent cohesion

c'= effective cohesion

b= angle of failure plane

$W_i sin\beta$= the component of soil weight down the failure plane, driving the soil downward

$W_i cos\beta tan\emptyset_i'$= frictional resisting of the soil along the failure plane.

$W_i cos\beta$=component of soil weight normal to failure plane

$\emptyset_i'$=friction angle of the soil

$c_i' L_i$=effective cohesion per unit length

$P_i \cos(\alpha - \beta)\ tan\emptyset_i'$=the normal component of the hydrostatic confining forces the water in the channel

$-P_i \sin[\alpha - \beta]$=the component of the hydrostatic confining forces acting along the failure plane

$U_i tan\emptyset_i'$=hydrostatic uplift force

$S_i tan\emptyset_i^b$=suction forces

b) Toe Erosion

The toe erosion module of BSTEM computes undermining of the bank toe as a result of fluvial erosion (Simon et al., 2000; Midgley et al., 2012). Excess shear stress formulation originally proposed by Partheniades (1965) is adopted to predict the erosion. Erosion rate, ε (m/s), is calculated as:

$$\varepsilon = k(\tau_0 - \tau_c)^a \qquad [6]$$

k is erodibility coefficient ($m^3N^{-1}S^{-1}$), $\tau_0 = \gamma RS$ is average shear stress (Nm^{-2}), τ_c is critical shear stress and a is exponent whose value is assumed as 1. The parameters k and τ_c depend on the properties of the soil. BSTEM divides the bank profiles into several nodes and for each of the nodes calculates τ_0 based on the flow segment affecting each node. Thus, a distribution of τ_0 is generated along the banks rather than just one average shear stress over the entire bank. To correct the boundary shear stress due to the effect of secondary flow in meandering channels, 'no-lag kinematic model' [**Eq. 7**] is used (Crosato, 2009).

$$\tau_0 = \frac{\gamma_w n^2 (u + U)^2}{R^{1/3}} \qquad [7]$$

Where, n is Manning's roughness coefficient, u is the channel-averaged flow velocity (m/s) and U is the increase in near-bank velocity due to super elevation (m/s)

6.3 Model Input and set-up

BSTEM requires river bathymetry, flow hydrographs and the soil parameters data as an input to calculate bank erosion analysis. The flow and the river bathymetry data is the same as mentioned in section 4. However, the measured data on riverbank soil parameters were unavailable. Accordingly, we had to choose from the default data available in the model. The soil parameters for the selected material type is presented in Table 1**.** Similarly, the soil-groundwater table data were also unavailable. Therefore we set the static groundwater level at 5m elevation.

Table 1: Soil parameters selected for the study reach [Adapted from (CEIWR-HEC, 2015)]

Default Bank material	Moderate soft clay
Saturated Unit weight (lb/ft^3)	112.7
Friction Angle, ϕ	26.4
Cohesion (lb/ft^2)	171.26
ϕ^b	15
Critical shear (lb/ft^2)	0.1044
Erodibility (ft^3/lb-s)	$2.86*10^{-4}$

6.4 Application in Uji River

Fig. 13 shows the evolution of cross-sections due to the erosion of banks after one year of simulation. It can be seen that toe erosion is dominant in cross-sections 1-3 whereas bank failure mode is more prominent in cross-section 1. The rate of bank erosion was higher in cross-sections 2-4 which may be due to their location along the bend. The distribution of bed shear stress in Fig.7 matches with the erosion locations. Fig. 14 compares the observed and simulated bank erosion rate. The predicted bank erosion rate closely matches the observed value at cross-sections 1 and 4. However, at sections 2 and 3, the model over predicted the erosion rate. This might be due to several factors. First, the bank material properties are assumed based on the default model data which could lead to uncertainty in the prediction. Similarly, the erosion rate is calculated as an average of the last 14 years of data. If we consider only the recent year's data, the predicted value will lie closer to the observed.

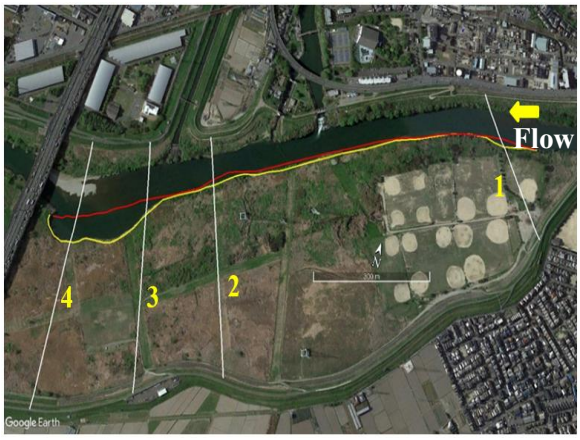

Fig.12: X-sections selected for bank erosion analysis

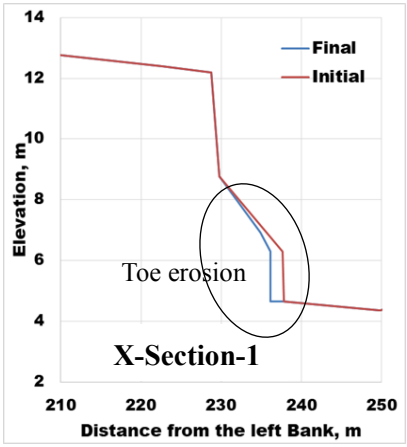

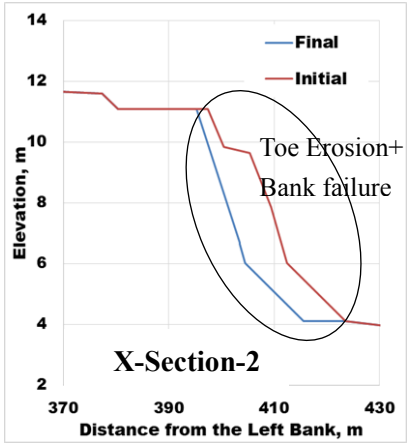

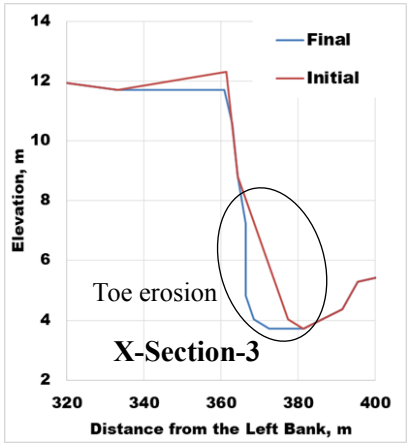

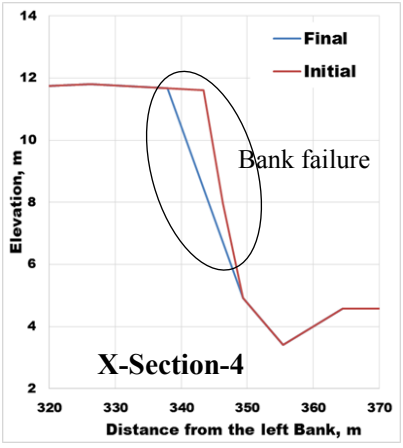

Fig.13 (a-d): Comparison of bank evolution at selected cross-sections

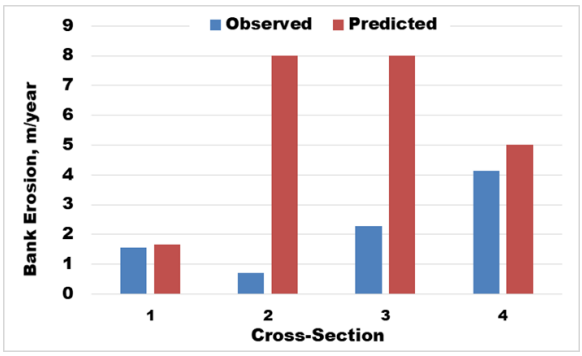

Fig.14: Comparison between the observed and the computed cross-sections

7. CONCLUSION & RECOMMENDATION

We performed numerical study of hydro-morphological characteristics of Uji River, Japan. The results showed that the overall channel evolution phenomena are not so dominant. However, the analysis of satellite images revealed that bank erosion at different locations has become serious. The results also signified that the low flow condition is more responsible for the continuous erosion of banks because it was observed that the near bank bed shear stress and velocity were greater during the low flow. However, the sediment data from the actual river couldn't be obtained. By incorporating further reliable data, we can improve the results in the future and also examine varieties of scenarios of bed and bank evolution for supporting the river management practitioners and the planners. Results of the prediction of bank erosion indicated that fluvial erosion due to the scour near the bank toe is dominant at most of the locations in Uji River. Finally, it is suggested that in the case of implementation of river bank protection works, research and analysis through simulation might help to select the optimum methods.

References

Ashida, K., Michiue, M. (1973): Studies on bed load transport rate in alluvial streams. Trans. JSCE 4

CEIWR-HEC (2015): HEC-RAS: USDA-ARS Bank Stability & Toe Erosion Model (BSTEM) Technical Reference & User's Manual 34.

Chang, H.H. (2008): River morphology and river

channel changes. Trans. Tianjin Univ. 14, 254–262.

Crosato, A.(2009): Physical explanations of variations in river meander migration rates from model comparison. Earth Surf. Process. Landforms 34, pp.2078–2086.

El Kadi Abderrezzak, K., Die Moran, A., Tassi, P., Ata, R., Hervouet, J.M. (2016): Modelling river bank erosion using a 2D depth-averaged numerical model of flow and non-cohesive, non-uniform sediment transport. Adv. Water Resour. 93, pp.75–88.

Engelund, F. (1974): Flow and bed topography in channel bends. J. Hydraul. Div. pp.1631–1648.

Hervouet, J.M., Bates, P. (2000): The telemac modelling system special issue. Hydrological Processes. Hydrol. Process. pp.2207–2208

Hirano, M. (1971): On river bed variation with armoring, in: Proceedings of the JSCE. pp. 55–65.

Koch, F., Flokstra, C. (1980): Bed level computations for curved alluvial channels. , New Delhi., in: Proceedings of the XIXth Congress of the Int. Ass. for Hydr. Res. New Delhi

Lagasse, P.F., Spitz, W.J., Zevenbergen, L.W. (2004): Handbook for predicting stream meander migration. Washington D.C.

Langendoen, E.J., Simon, A. (2008): Modeling the Evolution of Incised Streams. II: Streambank Erosion. J. Hydraul. Eng. 134, pp.905–915.

Midgley, T.L., Fox, G.A., Heeren, D.M. (2012): Evaluation of the bank stability and toe erosion model (BSTEM) for predicting lateral retreat on composite streambanks. Geomorphology 145–146, pp.107–114.

Simon, A., Bankhead, N., Thomas, R.E. (2010): Iterative bankstability and toe-erosion modeling for predicting streambank loading rates and potential load reductions, in: Paper Presented at Joint Federal Interagency Conference, Subcomm. on Hydrol. and Sediment., Advis. Comm. on Water Info. Las Vegas, Nevada

Simon, A., Curini, A., Darby, S.E., Langendoen, E.J. (2000): Bank and near-bank processes in an incised channel. Geomorphology 35, pp.183–217.

Villaret, C., Hervouet, J.M., Kopmann, R., Merkel, U., Davies, A.G. (2013): Morphodynamic modeling using the Telemac finite-element system. Comput. Geosci. 53, pp.105–113.

(Received June 17, 2019)